Alexandria Engineering Journal (2016) 55, 2125–2137

HOSTED BY

ELSEVIER

Alexandria University

Alexandria Engineering Journal

www.elsevier.com/locate/aej
www.sciencedirect.com

ORIGINAL ARTICLE

Soret and heat generation effects on MHD Casson fluid flow past an oscillating vertical plate embedded through porous medium

Hari R. Kataria [a], **Harshad R Patel** [b,*]

[a] *Department of Mathematics, Faculty of Science, The M. S. University of Baroda, Vadodara, India*
[b] *Applied Science & Humanities Department, Sardar Vallabhbhai Patel Institute of Technology, Vasad, India*

Received 26 April 2016; revised 10 June 2016; accepted 25 June 2016
Available online 18 July 2016

KEYWORDS

Magneto hydrodynamics;
Casson fluid;
Ramped temperature;
Skin friction: Nusselt number;
Sherwood number

Abstract Analytical solution of thermal diffusion and heat generation effects on MHD Casson fluid flow past an oscillating vertical plate embedded through porous medium in the presence of thermal radiation and chemical reaction is obtained. Ramped wall temperature with ramped surface concentration, isothermal temperature with ramped surface concentration and isothermal temperature with constant surface concentration are taken into account. The governing non-dimensional equations are solved using Laplace transform technique and the solutions are presented in closed form. In order to get a perfect understanding of the physics of the problem we obtained numerical results using Matlab software and clarified with the help of graphical illustrations. With the help of velocity, temperature and concentration, Skin friction, Nusselt number and Sherwood number are obtained and represent through tabular form. Casson parameter is inversely proportional to the yield stress and it is observed that for the large value of Casson parameter, the fluid is close to the Newtonian fluid where the velocity is less than the non-Newtonian fluid. The intensification in values of Soret number produces a raise in the mass buoyancy force which results an increase in the value of velocity.

1. Introduction

Magnetohydrodynamics is the study of the motion of the fluid in the presence of magnetic field. The study of MHD flows has great importance, as these flows are quite prevalent in nature. The application of MHD to natural events received a delayed motivation when astrophysicists came to realize how established throughout the universe conducting, ionized gases and significantly strong magnetic fields. First theory of laminar flow of an electrically conductive liquid in a homogenous magnetic field was introduced in 1937 by Hartman [1]. Huang [2] discussed MHD waves and instabilities in the heat-conducting solar wind plasma. Lee [3,4] studied energy of Alfvén waves generated during magnetic reconnection. Nadeem [5–7] defined analytic/numerical solution of free/mixed convection MHD flow of different fluid. Sheikholeslami [8,9] considered unsteady

* Corresponding author.
E-mail addresses: hrkrmaths@yahoo.com (H.R. Kataria), harshadpatel2@gmail.com (H.R Patel).

Peer review under responsibility of Faculty of Engineering, Alexandria University.

http://dx.doi.org/10.1016/j.aej.2016.06.024

Nomenclature

B_0	uniform magnetic field
C'	species concentration
D_M	mass diffusion coefficient
D_T	thermal diffusion coefficient
Gm	mass Grashof number
k_1	permeability parameter
k_1'	permeability of porous medium
Pr	Prandtl number
M	magnetic parameter
Sc	Schmidt number
u'	fluid velocity in x' direction
t'	time
q_r	radiative heat flux
R	thermal radiation
θ	dimensionless fluid temperature
u	dimensionless fluid velocity in x direction
C	dimensionless species concentration
C_p	specific heat at constant pressure
g	acceleration due to gravity
Gr	thermal Grashof number
Kr	chemical reaction parameter
Q_0	heat absorption/generation coefficient
T'	fluid temperature
t	dimensionless time
H	heat generation parameter
a	absorption constant

Greek symbols

$\varnothing$	porosity of the fluid
β_T'	volumetric coefficient of thermal expansion
β_c'	volumetric coefficient of species concentration expansion
$\mu\beta$	plastic dynamic viscosity
v	kinematic viscosity coefficient
ρ	fluid density
σ	electrical conductivity
γ	Casson parameter

free convective MHD flow with nano/ferro fluid with different boundary conditions. Rashidi [10,11] has discussed on steady/unsteady MHD and slip flow over a rotating porous disk. Hayat [12–14] has studied Soret and Dufour effects on one/three dimensional MHD flow with different fluid and boundary conditions. Hussnan [15,16] illustrates that free convective flow past an oscillating plate with Newtonian heating. Recently most of the researchers Ahmed [17], Narayana [18] and Abbas [19] worked on radiation and chemical reactions effects on MHD flow with different fluid with heat and mass transfer.

The theory of non-Newtonian fluid is a part of fluid mechanics based on the continuum theory that a fluid particle may be considered as continuous in a structure. Pseudo plastic time independent fluid is one of the non-newtonian fluids whose behavior is that Viscosity decreases with increasing velocity gradient e.g. polymer solutions, blood, etc. Casson fluid is one of the pseudoplastic fluids that means shear thinning fluids. At low shear rates the shear thinning fluid is more viscous than the Newtonian fluid, and at high shear rates it is less viscous. So, MHD flow with Casson fluid is recently famous. Casson [20] presented Casson fluid model for the prediction of the flow conduct of pigment-oil suspensions. Dash et al. [21] discussed on Casson fluid flow in a pipe with a homogeneous porous medium. Akbar [22–25] has studied Casson Fluid flow in a Plumb Duct/asymmetric channel. Mohyud-Din [26,27] has discussed on magnetic field and radiation effects on squeezing flow of a Casson fluid between parallel plates. Raju [28] has studied effect of induced magnetic field on stagnation flow of a Casson fluid. Kataria [29–31] published the work on unsteady free convective MHD Casson/micropolar/nano fluid flow with different boundary conditions. Recently, Makanda [32,33] has discussed effects on radiation as well as chemical reaction on Casson fluid flow. Abbasi [34–39] has considered three dimensional MHD flow with different fluid and different physical conditions.

Such effects are significant when density differences exist in the flow regime. For example when species are introduced at a surface in fluid domain, with different (lower) density than the surrounding fluid, Soret effects can be significant. Also, when heat and mass transfer occur simultaneously in a moving fluid, the relations between the fluxes and the driving potentials are of more complex nature. It has been found that an energy flux can be generated not only by temperature gradients but also by composition gradients as well. The thermal diffusion (Soret) effect, for instance, has been utilized for isotope separation, and in mixture between gases with very light molecular weight (H_2, He) and of medium molecular weight (N_2, air). In fluid mechanics, fluid flow through porous media is the manner in which fluids behave when flowing through a porous medium, for example sponge or wood, or when filtering water using sand or another porous material. As commonly observed, some fluid flows through the media while some mass of the fluid is stored in the pores present in the media. The basic law governing the flow of fluids through porous media is Darcy's Law.

Therefore our work can be considered as extension of Ref. [31]. So Novelty of this paper is discussion of analytical solutions using laplace transform and numerical solution using Matlab software (finite difference method) of the unsteady natural convective Casson fluid flow past over an oscillating vertical plate in the presence of a radiation, chemical reaction, thermal diffusion and heat generation with ramped wall temperature and ramped surface concentration through porous medium.

2. Mathematical formulation of the problem

In Fig. 1 the flow being confined to $y' > 0$, where y' the coordinate is measured in the normal direction to the plate and x'-axis is taken along the wall in the upward direction. Initially, at time $t' = 0$, both the fluid and the plate are uniform

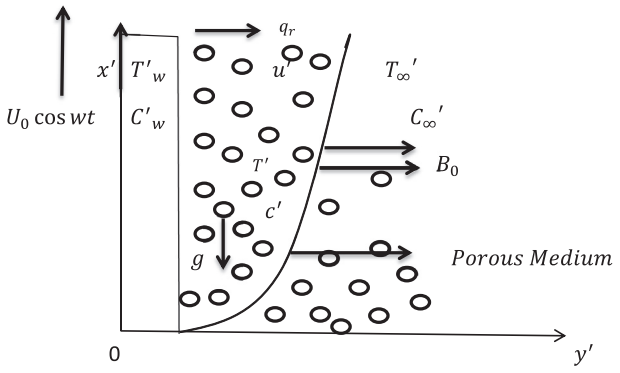

Figure 1 Physical sketch of the problem.

temperature T'_∞ and the concentration near the plate is assumed to be C'_∞ at all the points respectively. At time $t' > 0$, the plate is exponentially accelerated in the vertical direction against gravitational field with velocity $U_0 e^{a't}$ and constant heat flux, $T'_\infty + (T'_w + T'_\infty)t'/t_0$ when $t' \leqslant t_0$ and T'_w when $t' > t_0$ respectively which is thereafter maintained constant T'_w and the level of mass transfer at the surface of the plate is raised or lowered to $C'_\infty + (C'_w + C'_\infty)t'/t_0$ when $t' \leqslant t_0$ and C'_w when $t' > t_0$ respectively which is thereafter maintained constant C'_w. An uniformly magnetic field of strength B_0 is applied in the y'-axis direction. Induced magnetic field is negligible. We assume that, rigid plate, incompressible flow, one dimensional flow, non-Newtonian fluid, free convection and viscous dissipation term in the energy equation are neglected. Under these conditions we get the following partial differential equation with initial and boundary conditions:

$$\rho\frac{\partial u'}{\partial t'} = \mu_B\left(1+\frac{1}{\gamma}\right)\frac{\partial^2 u'}{\partial y^2} - \sigma B_0^2 u' - \frac{\mu\varphi}{k_1'}u' + \rho g\beta'_T(T'-T'_\infty) + \rho g\beta'_C(C'-C'_\infty) \tag{1}$$

$$\frac{\partial T'}{\partial t'} = \frac{k}{\rho c_p}\frac{\partial^2 T'}{\partial y'^2} - \frac{1}{\rho c_p}\frac{\partial q_r}{\partial y'} + \frac{Q_0}{\rho c_p}(T'-T'_\infty) \tag{2}$$

$$\frac{\partial C'}{\partial t'} = D_M\frac{\partial^2 C'}{\partial y'^2} + D_T\frac{\partial^2 T'}{\partial y'^2} - k_2'(C'-C'_\infty) \tag{3}$$

with following initial and boundary conditions:

$$u' = 0, \quad T' = T'_\infty, \quad C' = C'_\infty; \quad \text{as } y' \geqslant 0 \text{ and } t' \leqslant 0,$$
$$u' = U_0\cos wt/\sin wt, \quad \text{as } t' > 0 \text{ and } y' = 0,$$

$$T' = \begin{cases} T'_\infty + (T'_w - T'_\infty)t'/t_0 & \text{if } 0 < t' < t_0 \\ T'_w & \text{if } t' \geqslant t_0 \end{cases},$$
$$C' = \begin{cases} C'_\infty + (C'_w - C'_\infty)t'/t_0 & \text{if } 0 < t' < t_0 \\ C'_w & \text{if } t' \geqslant t_0 \end{cases}; \quad y' = 0$$

$$u' \to 0, \quad T' \to T'_\infty, \quad C' \to C'_\infty; \quad \text{as } y' \to \infty \text{ and } t' \geqslant 0 \tag{4}$$

As we have optically thick Casson fluid, we can use Rosseland approximation [40]

$$\frac{\partial q_r}{\partial y'} = -4a\sigma(T'^4_\infty - T'^4) \tag{5}$$

where a is absorption constant, T'^4 can be expanded as the linear temperature function. Using Taylor series expanding T'^4 about T'_∞ and neglecting higher order term, we get

$$T'^4 \cong 4T'^3_\infty T' - 3T'^4_\infty \tag{6}$$

where

$$y = \frac{y'}{U_0 t_0}, \quad u = \frac{u'}{U_0}, \quad t = \frac{t'}{t_0}, \quad \theta = \frac{(T'-T'_\infty)}{(T'_w - T'_\infty)},$$
$$C = \frac{(C'-C'_\infty)}{(C'_w - C'_\infty)}, \quad Gr = \frac{\nu g\beta'_T(T'_w - T'_\infty)}{U_0^3}$$

$$Gm = \frac{\nu g\beta'_C(C'_w - C'_\infty)}{U_0^3}, \quad M = \frac{\sigma B_0^2\nu}{\rho U_0^2}, \quad P_r = \frac{\rho\nu C_p}{k},$$
$$R = \frac{16a\sigma\nu^2 T'^3_\infty}{kU_0^2}, \quad H = \frac{Q_0\nu^2}{kU_0^2}, Sc = \frac{\nu}{D_M}$$

$$Kr = \frac{\nu k_2'}{U_0^2}, \quad Sr = \frac{D_T(T'_w - T'_\infty)}{\nu(C'_w - C'_\infty)}, \quad \gamma = \frac{\mu_B\sqrt{2\pi_c}}{P_y}, \quad \tau = \frac{\tau}{\rho u^2}$$

Substituting values from Eq. (5) and Eq. (6) in Eq. (3) and in Eqs. (1)–(3) and dropping out the "′" notation (for simplicity) we get

$$\frac{\partial u}{\partial t} = \left(1+\frac{1}{\gamma}\right)\frac{\partial^2 u}{\partial y^2} - \left(M^2 + \frac{1}{k}\right)u + G_r\theta + G_m C \tag{7}$$

$$\frac{\partial\theta}{\partial t} = \frac{1}{Pr}\frac{\partial^2\theta}{\partial y^2} + \frac{(H-R)}{Pr}\theta \tag{8}$$

$$\frac{\partial C}{\partial t} = \frac{1}{s_c}\frac{\partial^2 C}{\partial y^2} + Sr\frac{\partial^2\theta}{\partial y^2} - krC \tag{9}$$

with initial and boundary condition

$$u = \theta = C = 0, \quad y \geqslant 0, \quad t \leqslant 0, \quad u = \cos wt/\sin wt \text{ at } y = 0, \; t > 0,$$

$$\theta = \begin{cases} t, & 0 < t \leqslant 1 \\ 1 & t > 1 \end{cases}, \quad C = \begin{cases} t, & 0 < t \leqslant 1 \\ 1 & t > 1 \end{cases} \quad \text{at } y = 0, \; t > 0,$$
$$u \to 0, \; \theta \to 0, \; C \to 0 \text{ at } y \to \infty, \; t > 0 \tag{10}$$

Exact solution for fluid velocity, Temperature and Concentration are obtained from Eqs. (7)–(9) with initial and boundary conditions (10) using the Laplace transform technique.

2.1. Solution of the problem for ramped wall temperature and ramped surface concentration

$$\theta(y,t) = f_9(y,t) - f_9(y,t-1)H(t-1) \tag{11}$$

$$C(y,t) = h_2(y,t) - h_2(y,t-1)H(t-1) \tag{12}$$

$$u(y,t) = g_1(y,t) + h_1(y,t) - h_1(y,t-1)H(t-1) \tag{13}$$

2.2. Solution of the problem for isothermal temperature and ramped surface concentration

In order to understand effects of ramped temperature of the plate on the fluid flow, we must compare our results with

isothermal temperature. In this case, the initial and boundary conditions are the same excluding Eq. (10) that becomes $\theta = 1$ at $y = 0,\ t \geqslant 0$. We find the isothermal temperature $\theta(y,t)$ using Laplace transform.

$$\theta(y,t) = f_8(y,t) \tag{14}$$

$$C(y,t) = f_{13}(y,t) - f_{13}(y,t-1)H(t-1) + g_{12}(y,t) - g_{13}(y,t) \tag{15}$$

$$u(y,t) = g_1(y,t) + g_5(y,t) + g_6(y,t) - g_6(y,t-1)H(t-1) + g_7(y,t) - g_8(y,t) + g_8(y,t-1)H(t-1) - g_9(y,t) \tag{16}$$

2.3. Solution of the problem for isothermal temperature and constant surface concentration

In this case, the initial and boundary conditions are the same excluding Eq. (10) that becomes $C = 1,\ \theta = 1$ at $y = 0,\ t \geqslant 0$. We find the constant temperature and constant surface concentration $\theta(y,t)$ and $C(y,t)$ using Laplace transform.

$$\theta(y,t) = f_8(y,t) \tag{17}$$

$$C(y,t) = f_{12}(y,t) + g_{12}(y,t) - g_{13}(y,t) \tag{18}$$

$$u(y,t) = h_3(y,t) \tag{19}$$

2.4. Nusselt number, Sherwood number and Skin friction

Expressions of Nusselt number Nu, Sherwood Number Sh and Skin friction τ for all cases are calculated from Eqs. (11)–(19) respectively using the relation

$$N_u = -\frac{v}{U_0(T' - T'_\infty)}\left(\frac{\partial T'}{\partial y'}\right)_{y'=0}, s_h = -\frac{v}{U_0(C' - C'_\infty)}\left(\frac{\partial C'}{\partial y'}\right)_{y'=0}$$

$$\text{and} \quad \tau^*(y,t) = -\mu_B\left(1 + \frac{1}{\gamma}\right)\tau \text{ where } \tau = \left.\frac{\partial u}{\partial y}\right|_{y=0} \tag{20}$$

2.5. For ramped wall temperature and ramped surface concentration

$$Nu = -[J_9(t) - J_9(t-1)H(t-1)] \tag{21}$$

$$Sh = -[J_{32}(t) - J_{32}(t-1)H(t-1)] \tag{22}$$

$$\tau = J_{16}(t) + J_{31}(t) - J_{31}(t-1)H(t-1) \tag{23}$$

2.6. For isothermal temperature and constant surface concentration

$$Nu = -[J_8(t)] \tag{24}$$

$$Sh = -[J_{13}(t) - J_{13}(t-1)H(t-1) + J_{27}(t) - J_{28}(t)] \tag{25}$$

$$\tau = J_{16}(t) + J_{20}(t) + J_{21}(t) - J_{21}(t-1)H(t-1) + J_{22}(t) - J_{23}(t) + J_{23}(t-1)H(t-1) - J_{24}(t) \tag{26}$$

2.7. For isothermal temperature and constant surface concentration

$$Nu = -[J_8(t)] \tag{27}$$

$$Sh = -[J_{12}(t) + J_{27}(t) - J_{28}(t)] \tag{28}$$

$$\tau = J_{33}(t) \tag{29}$$

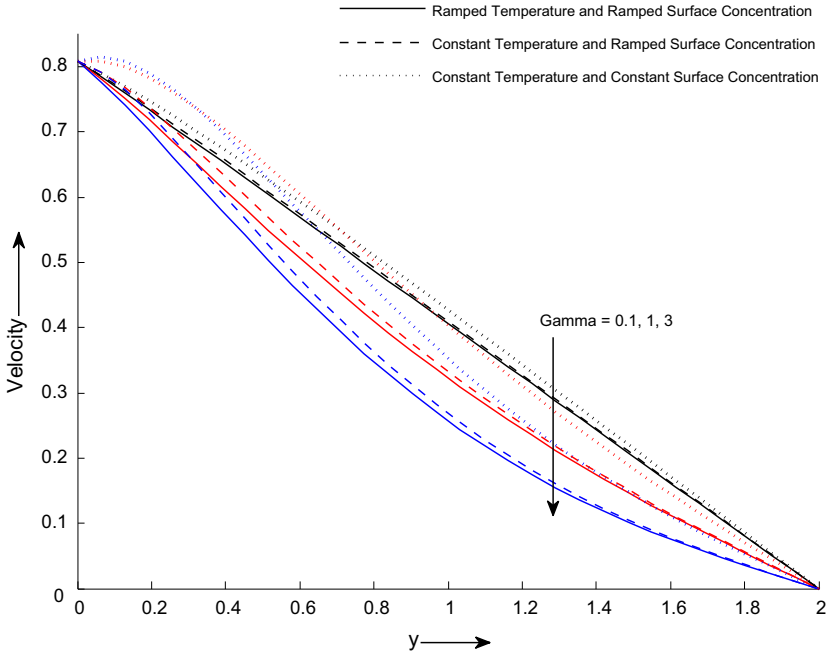

Figure 2 Velocity profile u for different values of y and γ at $Pr = 25$, $M = 0.5$, $k = 1$, $Sc = 0.66$, $Gm = 2$, $Gr = 4$, $R = 5$, $Kr = 4$, $H = 5$, $Sr = 7$ and $t = 0.4$.

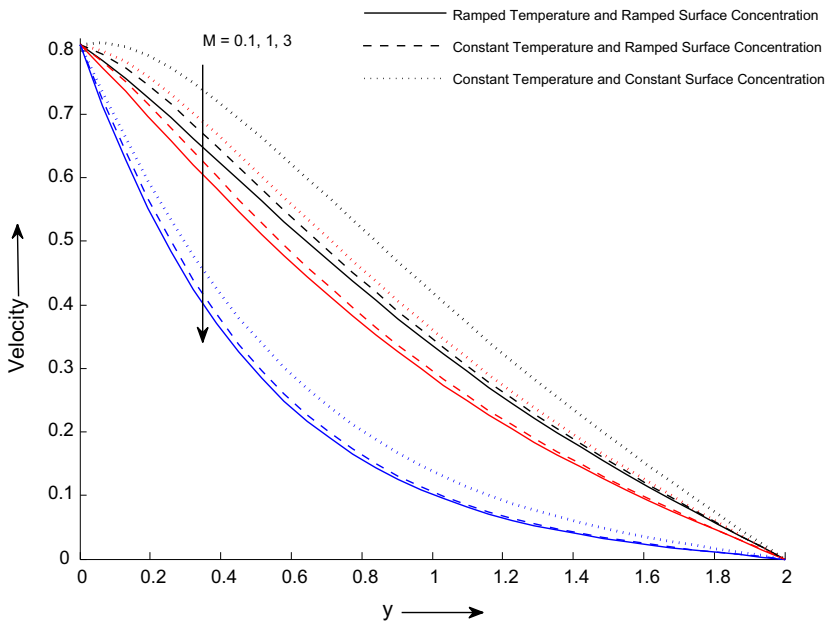

Figure 3 Velocity profile u for different values of y and M at $\gamma = 1$, $P = 25$, $k = 1$, $Sc = 0.66$, $Gm = 2$, $Gr = 4$, $R = 5$, $Kr = 4$, $H = 5$, $Sr = 7$ and $t = 0.4$.

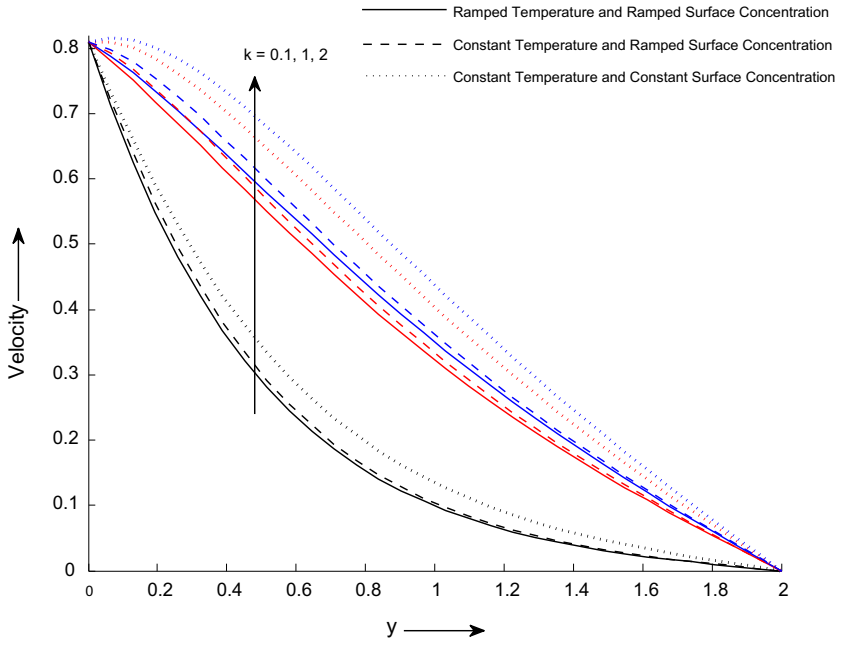

Figure 4 Velocity profile u for different values of y and k at $\gamma = 1$, $M = 0.5$, $Pr = 25$, $Sc = 0.66$, $Gm = 2$, $Gr = 4$, $R = 5$, $Kr = 4$, $H = 5$, $Sr = 7$ and $t = 0.4$.

3. Result and discussion

In order to study the influence of physical parameters, we find exact solution using Laplace transform and Numerical solution using Matlab software and present graphically through Figs. 2–12.

Effect of Casson fluid parameter γ on velocity profiles is shown in Fig. 2. It is found that velocity decreases with increasing values of γ. It is noticed that Casson parameter does not have any influence as the fluid moves away from the bounding surface. For the large value of Casson parameter, the fluid resembles to the Newtonian fluid where the velocity is less than the non-Newtonian fluid. It is also observed that the axial velocity at the surface is larger than the transverse velocity. Fig. 3 shows that velocity decreases with increase in M. This is due to the fact that the application of a magnetic field to an electrically conducting fluid gives rise to a resistive force called Lorentz force which has a tendency to slow down

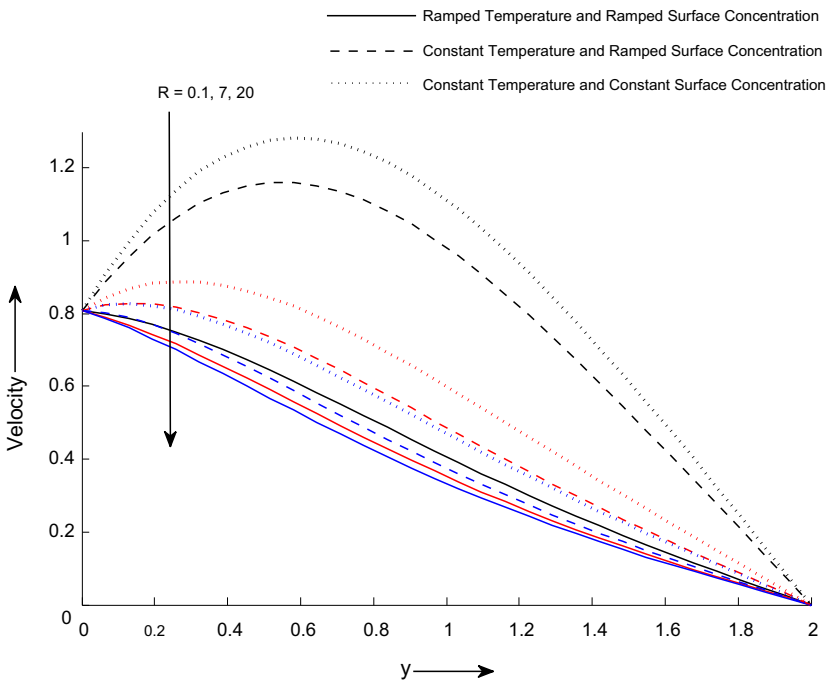

Figure 5 Velocity profile u for different values of y and R at $\gamma = 1$, $M = 0.5$, $k = 1$, $Sc = 0.66$, $Gm = 2$, $Pr = 0.71$, $R = 5$, $Kr = 4$, $H = 5$, $Sr = 7$ and $t = 0.4$.

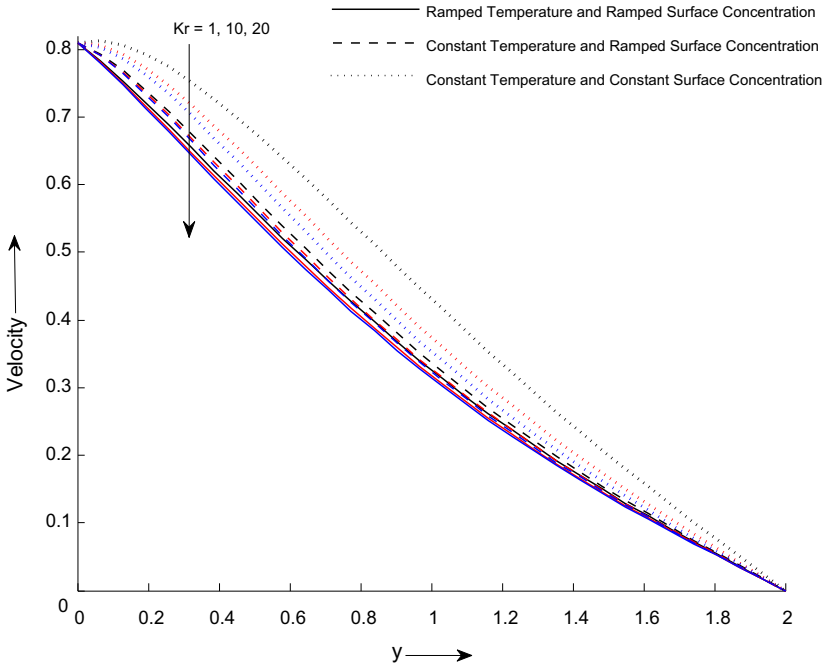

Figure 6 Velocity profile u for different values of y and Kr at $\gamma = 1$, $M = 0.5$, $k = 1$, $Sc = 0.66$, $Gm = 2$, $Gr = 4$, $R = 5$, $Pr = 25$, $H = 5$, $Sr = 7$ and $t = 0.4$.

the motion of fluid in the boundary layer region. Fig. 4 exhibits velocity profile for different values of porous medium k. If we increase porous medium parameter, holes become larger and therefor motion of the fluid rises. Hence velocity increases. Fig. 5 shows effect of radiation Parameter R on Velocity. It is observed that velocity has decreasing tendency with R. It is noticed that thermal radiation parameter reduces thermal buoyancy force, minimizing the thickness of the thermal boundary layer. Therefor velocity decreases tendency with radiation parameter R for all thermal cases. It can be seen that, with increased radiation in Casson fluid, heat transfer process is slow through the region. We compare the result with [31].

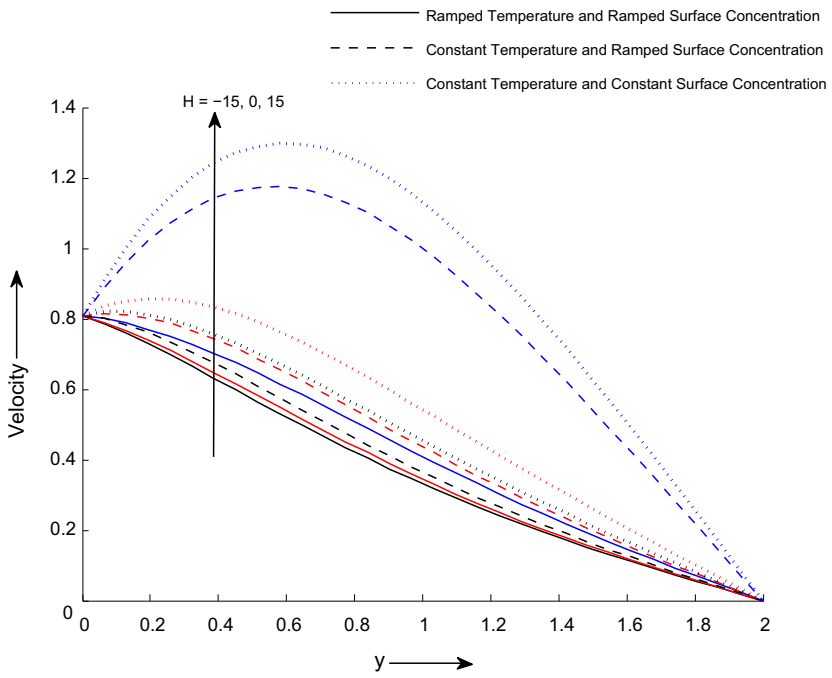

Figure 7 Velocity profile u for different values of y and H at $\gamma = 1$, $M = 0.5$, $k = 1$, $Sc = 0.66$, $Gm = 2$, $Gr = 4$, $R = 5$, $Pr = 0.71$, $H = 5$, $Sr = 7$ and $t = 0.4$.

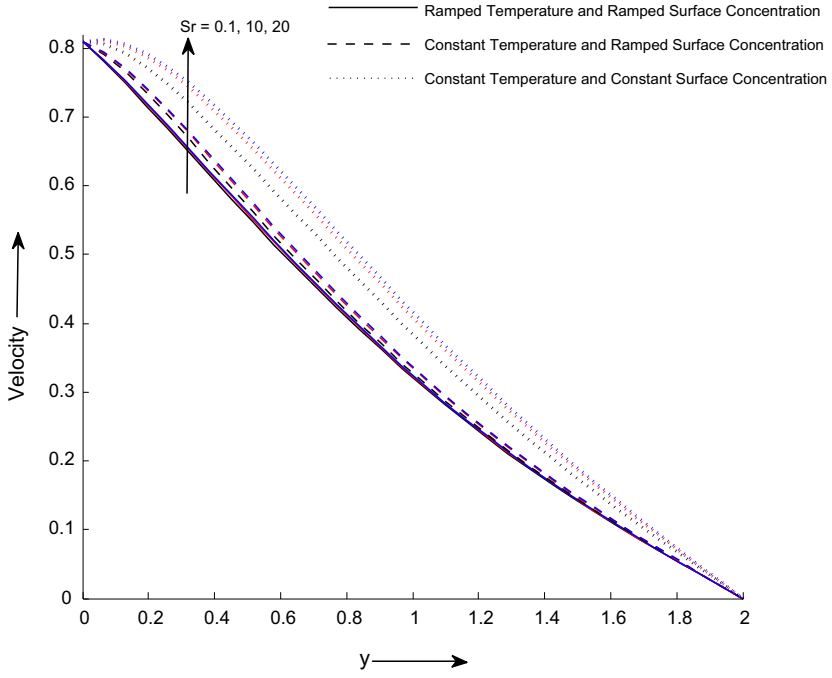

Figure 8 Velocity profile u for different values of y and Sr at $\gamma = 1$, $M = 0.5$, $k = 1$, $Sc = 0.66$, $Gm = 2$, $Gr = 4$, $R = 5$, $Kr = 4$, $H = 16$, $Pr = 25$ and $t = 0.4$.

Fig. 6 shows that velocity decreases with increase in chemical reaction parameter Kr. It is observed that the fluid motion is retarded on account of chemical reaction. We compared result with [31]. Effect of Heat generation parameter H on velocity is described in Fig. 7. It is noticed that Velocity has increasing tendency with H. Heat source implies generation of heat from the surface of the region, which raises the temperature in the flow field. Therefore, as heat generation parameter increases, the temperature increases as well as motion of the fluid is also increased. Fig. 8 exhibits effects of thermal-diffusion on veloc-

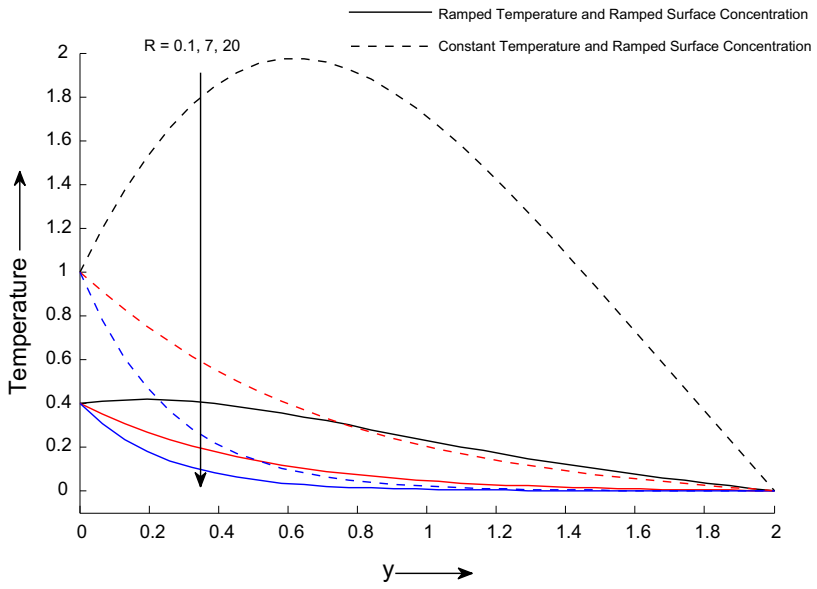

Figure 9 Temperature profile $u\ \theta$ for different values of y and R at $Pr = 0.71$, $H = 5$ and $t = 0.4$.

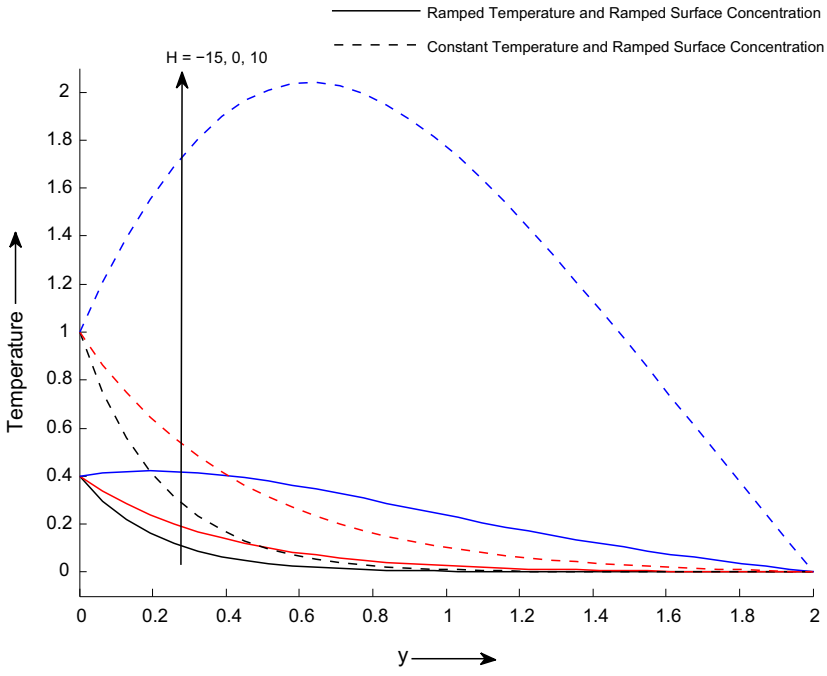

Figure 10 Temperature profile θ for different values of y and H at $R = 5$, $Pr = 0.71$ and $t = 0.4$.

ity for all thermal cases. It is observed from these figures that the velocity of the fluid gets accelerated by the rise in values of Soret number. Intensification in values of Soret number raises the mass buoyancy force which results an increase in the value of velocity. Fig. 9 shows effect of thermal radiation effects on temperature profile for both thermal plates. It is evident that temperature of the fluid decreases with increase in Radiation parameter. We compare result with [31]. Fig. 10 shows effect of Heat generation parameter H on temperature profile for ramped wall temperature with ramped surface concentration and isothermal temperature with constant surface concentration. For both thermal plates, Temperature increases with increase in heat generation parameter H. Fig. 11 shows that concentration decreases with increase in chemical reaction parameter Kr. This shows that the destructive reaction leads to decrease in the concentration field which in turn fails the buoyancy effects due to concentration gradients. We compare result with [31]. Fig. 12 indicates concentration profile for different values of thermal-diffusion for ramped wall temperature with ramped surface concentration, isothermal temperature with ramped surface concentration and constant temperature with constant surface concentration. For all cases, we illustrate that Soret number tends to increase concentration profile.

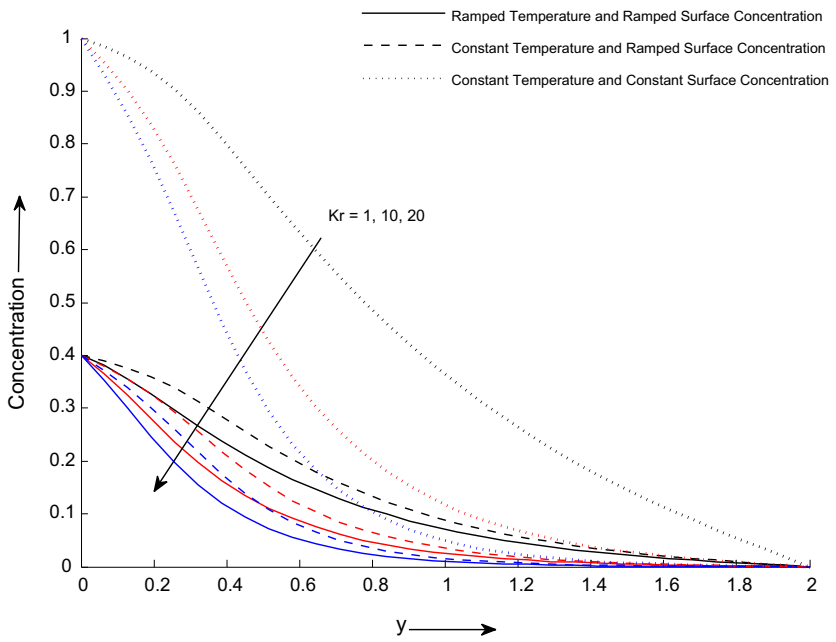

Figure 11 Concentration profile u for different values of y and Kr at $Gm = 2$, $Gr = 4$, $R = 5$, $Sc = 0.66$, $H = 5$, $Sr = 7$, $Pr = 25$ and $t = 0.4$.

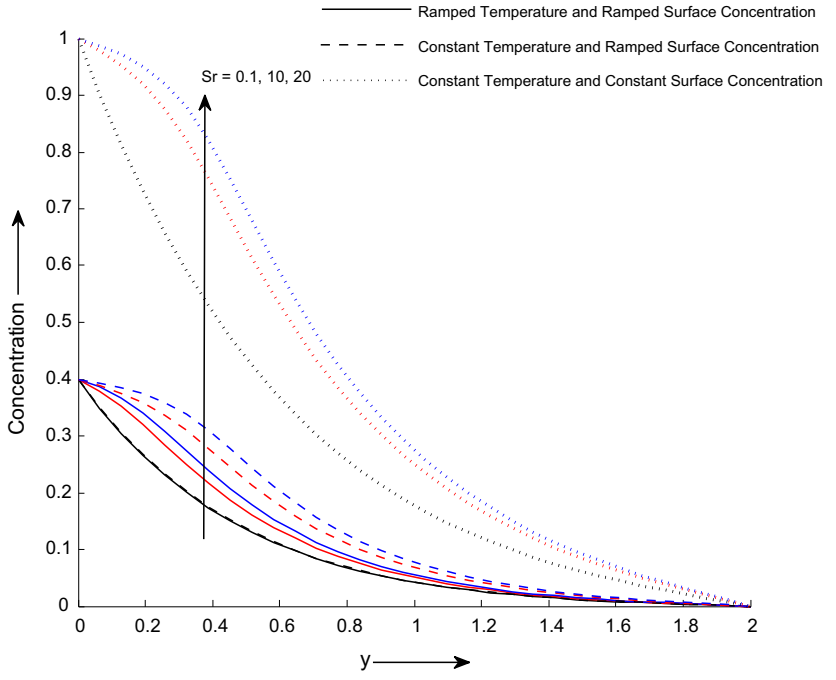

Figure 12 Concentration profile u for different values of y and Sr at $Gm = 2$, $Gr = 4$, $R = 5$, $Kr = 4$, $H = 5$, $Kr = 4$, $Pr = 25$ and $t = 0.4$.

The variations of the Skin friction, Nusselt number and Sherwood number are shown in Tables 1–3 for various values of the governing parameters. Table 2 shows the effect of Pr, H and time on temperature gradient on the surface. For all thermal cases, Prandtl number and Heat source parameter tend to reduce the magnitude of Nusselt number while time variable t tends to reverse process in it. Table 3 indicates the magnitude values of mass gradient at the surface. For all thermal cases, it is shown that thermal radiation and time variable t tend to reduce the values of Sherwood number while Soret number and Heat source parameter tend to reverse effect on it. Table 1 shows the effect of different physical parameter on shear stress. For all thermal cases, ramped wall temperature with ramped surface concentration, isothermal temperature with ramped surface concentration and constant temperature with constant surface concentration, magnitude of Skin friction decreases

Table 1 Skin friction variation.

γ	Sr	M	k	t	Skin friction τ for ramped temperature and ramped concentration	Skin friction τ for isothermal temperature and ramped concentration	Skin friction τ for constant temperature and constant concentration
0.1	0.2	0.1	1	0.4	−0.4813	−0.4779	−0.5548
0.15	0.2	0.1	1	0.4	−0.3481	−0.4018	−0.6887
0.2	0.2	0.1	1	0.4	−0.2580	−0.3587	−0.7975
0.1	0.3	0.1	1	0.4	−0.5503	−0.4807	−0.5576
0.1	0.4	0.1	1	0.4	−0.6194	−0.4834	−0.5604
0.1	0.2	0.2	1	0.4	−0.4679	−0.4669	−0.5574
0.1	0.2	0.3	1	0.4	−0.4475	−0.4502	−0.5617
0.1	0.2	0.1	1.1	0.4	−0.5284	−0.5165	−0.5469
0.1	0.2	0.1	1.2	0.4	−0.5774	−0.5567	−0.5403
0.1	0.2	0.1	1	0.5	−0.5891	−0.5765	−0.5557
0.1	0.2	0.1	1	0.6	−0.6960	−0.6735	−0.5601

Table 2 Nusselt number variation.

Pr	R	H	t	Nusselt number Nu for ramped temperature	Nusselt number Nu for isothermal temperature
15	7	5	0.4	0.1924	−2.9134
16	7	5	0.4	0.1866	−3.0433
17	7	5	0.4	0.1812	−3.1682
15	7.1	5	0.4	0.2018	−2.8869
15	7.2	5	0.4	0.2112	−2.8605
15	7	5.5	0.4	0.1451	−3.0467
15	7	6.0	0.4	0.0972	−3.1814
15	7	5	0.5	0.2675	−2.4878
15	7	5	0.6	0.3498	−2.1645

Table 3 Sherwood number variation.

R	Sr	H	t	Sherwood number Sh for ramped temperature and ramped concentration	Sherwood number Sh for isothermal temperature and ramped concentration	Sherwood number Sh for constant temperature and constant concentration
7	0.2	5	0.4	4.9522	0.1098	−0.2587
7.1	0.2	5	0.4	3.7547	0.1082	−0.2604
7.2	0.2	5	0.4	2.6888	0.1066	−0.2620
7	0.3	5	0.4	15.7829	0.1563	−0.2122
7	0.4	5	0.4	26.6137	0.2029	−0.1657
7	0.2	5.5	0.4	13.9757	0.1179	−0.2507
7	0.2	6.0	0.4	34.9673	0.1260	−0.2425
7	0.2	5	0.5	4.1610	0.0997	−0.2279
7	0.2	5	0.6	3.5609	0.0941	−0.2049

with increase in Sr and t. It is also seen that, for both thermal cases magnitude of Skin friction increases with increase in Casson parameter γ and magnetic field M while decreases with increase in porous medium k. For constant temperature and constant surface concentration, Skin friction decreases with γ and M while increases with k.

4. Conclusion

The purpose of this study was to obtain exact solutions for the unsteady natural convective Casson fluid flow past over an oscillating vertical plate in the presence of radiation, chemical reaction, thermal diffusion and heat generation with ramped wall temperature and ramped surface concentration through porous medium. The expressions for the velocity, Temperature, concentration, Skin friction, Nusselt number and Sherwood number have been obtained in exact form with the help of the Laplace transform method. To analyze the effects of the physical parameters on velocity, concentration and temperature profiles, we find numerical solution using Matlab software and presented graphically. The most important concluding remarks can be summarized as follows:

- It is observed that magnitude of momentum, heat and mass transfer in case of ramped temperature with ramped surface concentration is less than that of isothermal temperature with ramped surface concentration.
- It is observed that magnitude of momentum, heat and mass transfer in case of constant temperature with ramped surface concentration is less than that of constant temperature with constant surface concentration.
- Motion of fluid decreases tendency with Casson parameter γ, chemical reaction Kr, thermal radiation R and increases tendency with heat generation H and thermal diffusion Sr.
- Temperature decreases with thermal radiation parameter R and increases with Heat generation H.
- Concentration decreases tendency with chemical reaction parameter Kr and increases with Soret number Sr.

Appendix A

$a = 1 + \frac{1}{\gamma}$ $b = M^2 + \frac{1}{k}$ $c = Gr$

$d = Gm$ $a_6 = \frac{1}{Pr}$ $a_7 = \frac{H-R}{Pr}$

$a_8 = \frac{1}{Sc}$ $a_9 = Sr$ $a_{10} = Kr$

$a_{11} = \frac{a_8}{a_6}$ $a_{12} = \frac{a_7}{a_6}$ $a_{13} = a_{10} - a_{12}$

$b_{14} = a_{11} - 1$ $a_{14} = \frac{a_9}{a_6}$ $a_{15} = \frac{a_{13}}{b_{14}}$

$a_{16} = \frac{a_{14}}{b_{14}}$ $a_{17} = \frac{-a_{16}a_7}{a_{15}}$ $a_{18} = \frac{-a_{16}(a_{15}+a_7)}{a_{15}^2}$

$a_{19} = \frac{a_{16}(1-a_7)}{1+a_{15}} - a_{17} - \frac{a_{18}}{1+a_{15}}$ $a_{20} = \frac{a}{a_6}$ $a_{21} = \frac{a.a_7}{a_6}$

$b_{21} = a_{20} - 1$ $a_{22} = b + a_{21}$ $a_{23} = \frac{a_{22}}{b_{21}}$

$a_{24} = \frac{c}{b_{21}}$ $b_{24} = \frac{a}{a_8} - 1$ $a_{25} = \frac{aa_{10}}{a_8} + b$

$a_{26} = \frac{a_{25}}{b_{24}}$ $a_{27} = \frac{d}{b_{24}}$ $a_{28} = \frac{da_{16}}{b_{24}}$

$a_{29} = \frac{da_{16}}{b_{21}}$ $a_{30} = \frac{-a_{24}}{a_{23}}$ $a_{31} = \frac{a_{24}}{a_{23}^2}$

$a_{33} = \frac{-a_{27}}{a_{26}}$ $a_{34} = \frac{a_{27}}{a_{26}^2}$ $a_{32} = \frac{a_{24}}{1-a_{23}} - a_{30} - \frac{a_{31}}{1-a_{23}}$

$a_{36} = \frac{a_{28}a_7}{a_{15}a_{26}}$ $a_{37} = \frac{a_{28}(a_7+a_{15})}{a_{15}^2(a_{26}+a_{15})}$ $a_{35} = \frac{a_{27}}{1-a_{26}} - a_{33} - \frac{a_{34}}{1-a_{26}}$

$a_{38} = \frac{a_{28}(a_{26}-a_7)}{a_{26}^2(a_{26}+a_{15})}$ $a_{40} = \frac{a_{29}a_7}{a_{15}a_{23}}$ $a_{39} = \frac{a_{28}(1-a_7)}{(1-a_{26})(1+a_{15})} - a_{36} - \frac{a_{37}}{1+a_{15}} - \frac{a_{38}}{1-a_{26}}$

$a_{41} = \frac{a_{29}(a_7+a_{15})}{a_{15}^2(a_{23}+a_{15})}$ $a_{42} = \frac{a_{29}(a_{23}-a_7)}{a_{23}^2(a_{23}+a_{15})}$ $a_{43} = \frac{a_{29}(1-a_7)}{(1-a_{23})(1+a_{15})} - a_{40} - \frac{a_{41}}{1+a_{15}} - \frac{a_{42}}{1-a_{23}}$

$a_{44} = a_{32} + a_{35} + a_{39} - a_{43}$ $a_{45} = a_{30} + a_{33} + a_{36} - a_{40}$ $a_{46} = a_{31} - a_{42}$

$a_{47} = a_{35} + a_{38}$ $a_{48} = a_{37} - a_{41}$ $a_{49} = a_{43} - a_{32}$

$a_{50} = a_{40} - a_{30}$ $a_{51} = a_{42} - a_{31}$ $a_{52} = -a_{35} - a_{39}$

$a_{53} = -a_{33} - a_{36}$ $a_{54} = -a_{34} - a_{38}$ $a_{55} = \frac{-a_{28}(a_{15}+a_7)}{a_{15}(a_{26}+a_{15})}$

$a_{56} = \frac{a_{28}(a_{26}-a_7)}{a_{26}(a_{26}+a_{15})}$ $a_{57} = \frac{-a_{29}(a_{15}+a_7)}{a_{15}(a_{23}+a_{15})}$ $a_{58} = \frac{a_{29}(a_{23}-a_7)}{a_{23}(a_{23}+a_{15})}$

$a_{59} = a_{30} + a_{36} - a_{40}$ $a_{60} = -a_{30} - a_{58}$ $a_{61} = a_{55} - a_{57}$

$a_{62} = a_{30} + a_{58}$ $a_{63} = \frac{a_{16}(a_{15}+a_7)}{a_{15}}$ $a_{64} = a_{33} - a_{56}$

$F_1(y,s) = \frac{e^{-y\sqrt{\frac{s+b}{a}}}}{s+iw}$ $F_2(y,s) = \frac{e^{-y\sqrt{\frac{s+b}{a}}}}{s-iw}$ $F_3(y,s) = \frac{e^{-y\sqrt{\frac{s+b}{a}}}}{s}$

$F_4(y,s) = \frac{e^{-y\sqrt{\frac{s+b}{a}}}}{s^2}$ $F_5(y,s) = \frac{e^{-y\sqrt{\frac{s+b}{a}}}}{s-a_{23}}$ $F_6(y,s) = \frac{e^{-y\sqrt{\frac{s+b}{a}}}}{(s-a_{26})}$

$F_7(y,s) = \frac{e^{-y\sqrt{\frac{s+b}{a}}}}{(s+a_{15})}$ $F_8(y,s) = \frac{e^{-y\sqrt{\frac{s-a_7}{a_6}}}}{s}$ $F_9(y,s) = \frac{e^{-y\sqrt{\frac{s-a_7}{a_6}}}}{s^2}$

$F_{10}(y,s) = \frac{e^{-y\sqrt{\frac{s-a_7}{a_6}}}}{(s-a_{23})}$ $F_{11}(y,s) = \frac{e^{-y\sqrt{\frac{s-a_7}{a_6}}}}{(s+a_{15})}$ $F_{12}(y,s) = \frac{1}{s}e^{-y\sqrt{\frac{s-a_{10}}{a_8}}}$

$F_{13}(y,s) = \frac{1}{s^2}e^{-y\sqrt{\frac{s-a_{10}}{a_8}}}$ $F_{14}(y,s) = \frac{e^{-y\sqrt{\frac{s-a_{10}}{a_8}}}}{(s-a_{26})}$ $F_{15}(y,s) = \frac{e^{-y\sqrt{\frac{s-a_{10}}{a_8}}}}{(s+a_{15})}$

$f_i(y,t) = L^{-1}F_i(y,s)$, $i = 1$–15 $h_i(y,t) = L^{-1}H_i(y,s)$, $i = 1$–3 $g_i(y,t) = L^{-1}G_i(y,s)$, $i = 1$–15

$h_1 = g_2 + g_3 + g_4$ $h_2 = f_{13} + g_{10} + g_{11}$ $h_3 = g_1 + g_7 + g_{14} + g_{15}$

$g_1 = \frac{i}{2}f_1 - \frac{i}{2}f_2$ $g_6 = a_{35}f_3 + a_{33}f_4 + a_{34}f_6$ $g_2 = a_{44}f_3 + a_{45}f_4 + a_{46}f_5 + a_{47}f_6 + a_{48}f_7$

$g_{11} = a_{19}f_8 + a_{17}f_9 + a_8f_{11}$ $g_5 = a_{59}f_3 + a_{60}f_5 + a_{61}f_7 + a_{56}f_6$ $g_3 = a_{49}f_8 + a_{50}f_9 + a_{51}f_{10} + a_{41}f_{11}$

$g_{12} = a_{17}f_{12} + a_{63}f_{15}$ $g_7 = a_{50}f_8 + a_{62}f_{10} + a_{57}f_{11}$ $g_4 = a_{52}f_{12} + a_{53}f_{13} + a_{54}f_{14} - a_{37}f_{15}$

$g_{13} = a_{17}f_8 + a_{63}f_{11}$ $g_8 = a_{35}f_{12} + a_{33}f_{13} + a_{34}f_{14}$ $g_9 = a_{36}f_{12} + a_{55}f_{15} + a_{56}f_{14}$

$g_{15} = a_{53}f_{12} - a_{55}f_{15} - a_{64}f_{14}$ $g_{10} = a_{19}f_{12} + a_{17}f_{13} + a_8f_{15}$ $g_{14} = a_{45}f_3 + a_{60}f_5 + a_{64}f_6 + a_{61}f_7$

$J_1 = \frac{df_1}{dy}\Big|_{y=0}$ ..... $J_{15} = \frac{df_{13}}{dy}\Big|_{y=0}$ $J_{16} = \frac{dg_1}{dy}\Big|_{y=0}$ ... $J_{30} = \frac{dg_{15}}{dy}\Big|_{y=0}$ $J_{31} = \frac{dh_1}{dy}\Big|_{y=0}$ ..... $J_{33} = \frac{dh_3}{dy}\Big|_{y=0}$

$$L^{-1}\left(\frac{e^{-y\sqrt{s+b}}}{s}\right)=\frac{1}{2}\left[e^{-y\sqrt{b}}erfc\left(\frac{y}{2\sqrt{t}}-\sqrt{bt}\right)+e^{y\sqrt{b}}erfc\left(\frac{y}{2\sqrt{t}}+\sqrt{bt}\right)\right]$$

$$L^{-1}\left(\frac{e^{-y\sqrt{s+b}}}{s^2}\right)=\frac{1}{2}\left[\left(t-\frac{y}{2\sqrt{b}}\right)e^{-y\sqrt{b}}erfc\left(\frac{y}{2\sqrt{t}}-\sqrt{bt}\right)+\left(t+\frac{y}{2\sqrt{b}}\right)e^{y\sqrt{b}}erfc\left(\frac{y}{2\sqrt{t}}+\sqrt{bt}\right)\right]$$

$$L^{-1}\left(\frac{e^{-y\sqrt{s+b}}}{(s+a)}\right)=\frac{e^{-at}}{2}\left[e^{-y\sqrt{\frac{1}{a}(b-a)}}erfc\left(\frac{y}{2\sqrt{t}}-\sqrt{(b-a)t}\right)+e^{y\sqrt{\frac{1}{a}(b-a)}}erfc\left(\frac{y}{2\sqrt{t}}+\sqrt{(b-a)t}\right)\right]$$

References

[1] J. Hartmann, Hg-dynamics I theory of the laminar flow of an electrically conductive liquid in a homogenous magnetic field, Det Kongelige Danske Videnskabernes Selskab Mathematisk-fysiske Meddeleser XV (1937) 1–27.

[2] L. Huang, L.C. Lee, Y.C. Whang, Magnetohydrodynamic waves and instabilities in the heat-conducting solar wind plasma, Planet. Space Sci. 36 (1988) 775–783.

[3] L.C. Lee, Time-dependent magnetic reconnection: two- and three-dimensional MHD simulations, Comput. Phys. Commun. 59 (1990) 163–174.

[4] L.C. Wang, L.J. Li, Z.W. Ma, X. Zhang, L.C. Lee, Energy of Alfvén waves generated during magnetic reconnection, Phys. Lett. A 379 (2015) 2068–2072.

[5] S. Nadeem, N.S. Akbar, Influence of radially varying MHD on the peristaltic flow in an annulus with heat and mass transfer, J. Taiwan Inst. Chem. Eng. 41 (2010) 286–294.

[6] S. Nadeem, S. Saleem, Analytical treatment of unsteady mixed convection MHD flow on a rotating cone in a rotating frame, J. Taiwan Inst. Chem. Eng. 44 (2013) 596–604.

[7] N.S. Akbar, S. Nadeem, R. Haq, S. Ye, MHD stagnation point flow of Carreau fluid toward a permeable shrinking sheet: dual solutions, Ain Shams Eng. J. 5 (2014) 1233–1239.

[8] M. Sheikholeslami, D.D. Ganji, M. Gorji-Bandpy, S. Soleimani, Magnetic field effect on nanofluid flow and heat transfer using KKL model, J. Taiwan Inst. Chem. Eng. 45 (2014) 795–807.

[9] M. Sheikholeslami, M. Gorji-Bandpy, D.D. Ganji, MHD free convection in an eccentric semi-annulus filled with nanofluid, J. Taiwan Inst. Chem. Eng. 45 (2014) 1204–1216.

[10] M.M. Rashidi, N. Kavyani, S. Abelman, Investigation of entropy generation in MHD and slip flow over a rotating porous disk with variable properties, Int. J. Heat Mass Transfer 70 (2014) 892–917.

[11] M.M. Rashidi, N.V. Ganesh, A.K. Abdul, B. Ganga, Buoyancy effect on MHD flow of nanofluid over a stretching sheet in the presence of thermal radiation, J. Mol. Liq. 190 (2014) 234–238.

[12] T. Hayat, S.A. Shehzad, A. Alsaedi, MHD three-dimensional flow of Maxwell fluid with variable thermal conductivity and heat source/sink, Int. J. Numer. Meth. Heat Fluid Flow 24 (5) (2014) 1073–1085.

[13] T. Hayat, H. Yasmin, M. Al-Yami, Soret and Dufour effects in peristaltic transport of physiological fluids with chemical reaction: a mathematical analysis, Comput. Fluids 89 (2014) 242–253.

[14] T. Hayat, Q.M. Rafiq, F. Alsaadi, M. Ayub, Soret and Dufour effects on peristaltic transport in curved channel with radial magnetic field and convective conditions, J. Magn. Magn. Mater. 405 (2016) 358–369.

[15] A. Hussnan, Z. Ismail, I. Khan, S. Shafie, Unsteady MHD free convection flow in a porous medium with constant mass diffusion and Newtonian heating, Euro. Phys. J. – Plus 129 (2014) 46.

[16] A. Hussnan, M. Anwar, F. Ali, I. Khan, S. Shafie, Natural convection flow past an oscillating plate with Newtonian heating, Heat Transfer Res. 45 (2014) 119–137.

[17] S. Ahmed, A. Mahdy, Unsteady MHD double diffusive convection in the stagnation region of an impulsively rotating sphere in the presence of thermal radiation effect, J. Taiwan Inst. Chem. Eng. 58 (2016) 173–180.

[18] P. Narayana, D. Babu, Numerical study of MHD heat and mass transfer of a Jeffrey fluid over a stretching sheet with chemical reaction and thermal radiation, J. Taiwan Inst. Chem. Eng. 59 (2016) 18–25.

[19] Z. Abbas, T. Javed, M. Sajid, N. Ali, Unsteady MHD flow and heat transfer on a stretching sheet in a rotating fluid, J. Taiwan Inst. Chem. Eng. 41 (2010) 644–650.

[20] N. Casson, A flow equation for the pigment oil suspensions of the printing ink type, in: Rheology of Disperse Systems, Pergamon, New York, 1959, pp. 84–102.

[21] R. Dash, K. Mehta, G. Jayaraman, Casson fluid flow in a pipe filled with a homogeneous porous medium, Int. J. Eng. Sci. 34 (1996) 1145–1156.

[22] N.S. Akbar, Influence of magnetic field on peristaltic flow of a Casson fluid in an asymmetric channel: application in crude oil refinement, J. Magn. Magn. Mater. 378 (2015) 463–468.

[23] N.S. Akbar, A. Butt, Physiological transportation of Casson fluid in a plumb duct, Commun. Theor. Phys. 63 (2015) 347–352.

[24] S. Nadeem, R. Ul Haq, N.S. Akbar, Z.H. Khan, MHD three-dimensional Casson fluid flow past a porous linearly stretching sheet, Alex. Eng. J. 52 (2013) 577–582.

[25] S. Nadeem, R. Ul Haq, N.S. Akbar, MHD three-dimensional boundary layer flow of Casson nanofluid past a linearly stretching sheet with convective boundary condition, IEEE Trans. Nanotechnol. 13 (2014) 109–115.

[26] S. Mohyud-Din, I. Khan, Nonlinear radiation effects on squeezing flow of a Casson fluid between parallel disks, Aerosp. Sci. Technol. 48 (2016) 186–192.

[27] A. Naveed, U. Khan, I. Khan, S. Bano, S. Mohyud-Din, Effects on magnetic field in squeezing flow of a Casson fluid between parallel plates, J. King Saud Univ. –Sci., doi:http://dx.doi.org/10.1016/j.jksus.2015.03.006.

[28] C.S.K. Raju, N. Sandeep, S. Saleem, Effects of induced magnetic field and homogeneous–heterogeneous reactions on stagnation flow of a Casson fluid, Eng. Sci. Technol., Int. J., doi: http://dx.doi.org/10.1016/j.jestch.2015.12.004.

[29] H. Kataria, A. Mittal, Mathematical model for velocity and temperature of gravity-driven convective optically thick nanofluid flow past an oscillating vertical plate in presence of magnetic field and radiation, J. Nig. Math. Soc. 34 (2015) 303–317.

[30] H. Kataria, H. Patel. Effect of magnetic field on unsteady natural convective flow of a micropolar fluid between two vertical walls, Ain Shams Eng. J., doi:http://dx.doi.org/10.1016/j.asej.2015.08.013.

[31] H. Kataria, H. Patel, Radiation and chemical reaction effects on MHD Casson fluid flow past an oscillating vertical plate embedded in porous medium, Alex. Eng. J. 55 (2016) 583–595.
[32] G. Makanda, S. Shaw, P. Sibanda, Effects of radiation on MHD free convection of a Casson fluid from a horizontal circular cylinder with partial slip in non-Darcy porous medium with viscous dissipation, Bound. Value Prob. 1 (2015) 1–14.
[33] G. Makanda, S. Shaw, P. Sibanda, Diffusion of chemically reactive species in Casson fluid flow over an unsteady stretching surface in porous medium in the presence of a magnetic field, Math. Prob. Eng. (2015) 724596, http://dx.doi.org/10.1155/2015/724596.
[34] F. Abbasi, S. Shehzad, Heat transfer analysis for three-dimensional flow of Maxwell fluid with temperature dependent thermal conductivity: application of Cattaneo-Christov heat flux model, J. Mol. Liq. 220 (2016) 848–854.
[35] T. Hayat, T. Muhammad, S. Shehzad, A. Alsaedi, On three-dimensional boundary layer flow of Sisko nanofluid with magnetic field effects, Adv. Powder Technol. 27 (2016) 504–512.
[36] F. Abbasi, S. Shehzad, T. Hayat, B. Ahmad, Doubly stratified mixed convection flow of Maxwell nanofluid with heat generation/absorption, J. Magn. Magn. Mater. 404 (2016) 159–165.
[37] S. Shehzad, T. Hayat, A. Alsaedi, Three-dimensional MHD flow of Casson fluid in porous medium with heat generation, J. Appl. Fluid Mech. 9 (2016) 215–223.
[38] S. Shehzad, Z. Abdullah, A. Alsaedi, F.M. Abbasi, T. Hayat, Thermally radiative three-dimensional flow of Jeffrey nanofluid with internal heat generation and magnetic field, J. Magn. Magn. Mater. 397 (2016) 108–114.
[39] S. Shehzad, Z. Abdullah, F.M. Abbasi, T. Hayat, A. Alsaedi, Magnetic field effect in three-dimensional flow of an Oldroyd-B nanofluid over a radiative surface, J. Magn. Magn. Mater. 399 (2016) 97–108.
[40] S. Rosseland, Astrophysik und atom-theoretische Grundlagen, Springer-Verlag, Berlin, 1931.